




SARS-CoV-2's brain impact: revealing cortical and cerebellar differences via cluster analysis in COVID-19 recovered patients

Angel Omar Romero-Molina^{1,2} · Gabriel Ramirez-Garcia² · Amanda Chirino-Perez² · David Alejandro Fuentes-Zavaleta² · Carlos Roberto Hernandez-Castillo¹ · Oscar Marrufo-Melendez³ · Diana Lopez-Gonzalez⁴ · Mónica Rodriguez-Rodriguez⁴ · Armando Castorena-Maldonado⁴ · Yaneth Rodriguez-Agudelo³ · Francisco Paz-Rodriguez³ · Mireya Chavez-Oliveros³ · Susana Lozano-Tovar³ · Alonso Gutierrez-Romero³ · Antonio Arauz-Gongora³ · Raul Anwar Garcia-Santos³ · Juan Fernandez-Ruiz^{1,2} 

Received: 12 October 2023 / Accepted: 12 December 2023
© Fondazione Società Italiana di Neurologia 2024

Abstract

Background COVID-19 is a disease known for its neurological involvement. SARS-CoV-2 infection triggers neuroinflammation, which could significantly contribute to the development of long-term neurological symptoms and structural alterations in the gray matter. However, the existence of a consistent pattern of cerebral atrophy remains uncertain.

Objective Our study aimed to identify patterns of brain involvement in recovered COVID-19 patients and explore potential relationships with clinical variables during hospitalization.

Methodology In this study, we included 39 recovered patients and 39 controls from a pre-pandemic database to ensure their non-exposure to the virus. We obtained clinical data of the patients during hospitalization, and 3 months later; in addition we obtained T1-weighted magnetic resonance images and performed standard screening cognitive tests.

Results We identified two groups of recovered patients based on a cluster analysis of the significant cortical thickness differences between patients and controls. Group 1 displayed significant cortical thickness differences in specific cerebral regions, while Group 2 exhibited significant differences in the cerebellum, though neither group showed cognitive deterioration at the group level. Notably, Group 1 showed a tendency of higher D-dimer values during hospitalization compared to Group 2, prior to *p*-value correction.

Conclusion This data-driven division into two groups based on the brain structural differences, and the possible link to D-dimer values may provide insights into the underlying mechanisms of SARS-COV-2 neurological disruption and its impact on the brain during and after recovery from the disease.

Keywords COVID-19 · Cortical thickness · Inflammatory markers · Cognitive performance · Cluster analysis

Introduction

COVID-19 was initially described as primarily a respiratory infection caused by the SARS-CoV-2 virus [1]. However, subsequent reports have revealed the disease's clinical heterogeneity, encompassing a spectrum of manifestations across various systems, including gastrointestinal, cardiovascular, cutaneous [2, 3], and neurological [4] domains. Furthermore, persistent symptoms post-infection have been documented, marked by sensory and motor disturbances, with prominent symptoms including dizziness, vertigo, headache, cerebrovascular disease, seizures, anosmia, dysgeusia, fatigue, and myopathic pain [5–7]. In addition to these neurological alterations, COVID-19

✉ Raul Anwar Garcia-Santos
rawar33@gmail.com

✉ Juan Fernandez-Ruiz
jfr@unam.mx

¹ Instituto de Neurootologia, Universidad Veracruzana, Xalapa, Veracruz, Mexico

² Laboratorio de Neuropsicología, Facultad de Medicina, Universidad Nacional Autónoma de México, Mexico City, Mexico

³ Instituto Nacional de Neurología y Neurocirugía-INNN, Mexico City, Mexico

⁴ Instituto Nacional de Enfermedades Respiratorias-INER, Mexico City, Mexico

has been associated with deficits in cognitive performance [8] as well as in brain integrity, manifesting as long-term alterations in gray and white matter [9, 10].

Various hypotheses aim to elucidate the mechanism through which the virus induces alterations in the central nervous system (CNS). These hypotheses encompass direct invasion via routes such as the olfactory nerve [11] or the vagus nerve [12], the formation of microthrombi [13–15], or changes in blood–brain barrier permeability, associated with neuroinflammation [16]. In that sense, the neuroinflammatory process has been recognized as playing a pivotal role in the persistence of neurological symptoms [17] and structural changes in gray matter [18].

The pronounced peripheral inflammatory response, occurring acutely during the in-hospital phase when the infection reaches its peak, may potentially lead to widespread neuronal loss and an exacerbation of glia-mediated neuroinflammation that persists even after recovery from infection [19]. Likewise, the acute cytokine storm is considered to trigger severe brain damage that can extend to later stages of the disease [20]. Biochemical indicators that undergo alterations during the course of the infection include leukocytosis or leukopenia [21], elevated C-reactive protein, erythrocyte sedimentation rate, lactate dehydrogenase [22], interleukins [23, 24], and biomarkers associated with thrombosis — platelets, fibrinogen, and D-dimer [25–27] — that are linked with neuroinflammation processes.

The effect of SARS-CoV-2 infection on the brain is demonstrated by the persistent gray matter changes in patients who have recovered from COVID-19 and were followed up for 3 months [28]. Notably, the most affected brain regions include the frontal lobes, followed by the parietal, temporal, occipital, and even cerebellar areas [29]. However, the diversity of findings underscores the absence of a consistent pattern of cerebral atrophy across patients. In other words, the magnitude of cerebral atrophy in patients has been shown to be heterogeneous [30], and neurological alterations may be associated with the degree and location of long-term cerebral atrophy [31, 32]. In light of this, it is essential to establish potential connections between sustained cerebral impairment in individuals recovering from COVID-19 and quantified inflammatory markers and clinical-behavioral performance during the acute in-hospital phase of the disease. Therefore, the objectives of this study include: (1) characterizing the cortical integrity of cerebral and cerebellar regions in COVID-19 patients; (2) determining potential profiles of cerebral atrophy based on cortical thickness integrity; (3) exploring the possible relationship between cognitive scores, biomarkers, and their impact on cortical integrity in recovered COVID-19 patients.

Materials and methods

Participants

This study included 39 participants (28 males and 11 females) with an average age of 55.80 ± 9.34 years (*mean* \pm *SD*), who were admitted to the inpatient area of the Instituto Nacional de Enfermedades Respiratorias (INER) in Mexico City. These participants underwent clinical monitoring during their in-hospital stay, meeting the following inclusion criteria: hospitalization at the INER, positive polymerase chain reaction (PCR) test, age between 18 and 70 years, no history of neurological or psychiatric disorders, completion of a magnetic resonance imaging (MRI) study 3 months later, and completion of cognitive assessments. For each patient, a comprehensive dataset was compiled during hospitalization including comorbidities, symptoms reported upon admission, and pneumonia severity and oxygen therapy (Table 1). The clinical biochemical data including blood biochemistry, inflammatory markers, and coagulation factor measurements were obtained at the beginning of hospitalization. One participant lacked available clinical data and consequently was excluded from any analyses involving clinical variables, resulting in a total of 38 participants. As this study was carried out during the first wave of infections in Mexico, the emergence of new virus variants had not yet transpired, and vaccines and pharmacological treatments had not been developed; in this sense, they were not considered as variables in this study. Additionally, a control group of 39 subjects was included from a pre-pandemic database to ensure their non-exposure to the virus or asymptomatic infection (26 males and 13 females), with an average age of 55.15 ± 9.95 years. This control group only served for cerebral integrity comparisons and did not undergo evaluation for inflammatory markers or cognitive performance. The control group had no history of neurological or psychiatric disorders. All subjects were age- and sex-matched to the recovered COVID-19 patients. This project was approved by the research and ethical committee of the INER under approval number C48-20 and the Instituto Nacional de Neurología y Neurocirugía (INNN) under approval number 06–21. The procedures for human research adhered to the Helsinki Declaration.

Magnetic resonance imaging acquisition

The patients underwent T1-weighted MRI acquisition 3 months after hospital discharge [28]. This imaging procedure was conducted at the INNN, between February 22 and June 15, 2021, corresponding to Mexico's first

Table 1 COVID-19 patients' demographic data and reported symptoms on admission, and their subsequent grouping after hierarchical cluster analysis

| | All patients (<i>n</i> = 39) | Cluster analysis of cortical thickness | |
|---|-------------------------------|--|--------------------------|
| | | Group 1 (<i>n</i> = 22) | Group 2 (<i>n</i> = 17) |
| Age at examination, <i>mean</i> (\pm <i>SD</i>) | 55.8 (\pm 9.34) | 57.93 (\pm 7.28) | 53.05 (\pm 11.1) |
| Education, <i>mean</i> (\pm <i>SD</i>) | 11.41 (\pm 4.24) | 11.63 (\pm 4.55) | 11.23 (\pm 3.94) |
| Comorbidities, <i>n</i> (%) | | | |
| Diabetes | 14 (35.89) | 7 (31.81) | 7 (41.17) |
| Hypertension | 10 (25.64) | 8 (36.36) | 2 (11.76) |
| Smoking | 0 (0) | 0 (0) | 0 (0) |
| Pulmonary disease | 7 (17.94) | 4 (18.18) | 3 (17.64) |
| Obesity | 16 (41.02) | 8 (36.36) | 8 (47.05) |
| Cardiovascular disease | 2 (5.12) | 2 (9.09) | 0 (0) |
| Reported symptoms on admission, <i>n</i> (%) | | | |
| Vertigo | 12 (30.76) | 8 (36.36) | 4 (23.52) |
| Anosmia | 5 (12.82) | 4 (18.18) | 1 (5.88) |
| Dysgeusia | 8 (20.51) | 7 (31.81) | 1 (5.88) |
| Headache | 9 (23.07) | 7 (31.81) | 2 (11.76) |
| Myopathic pain | 33 (84.61) | 18 (81.81) | 15 (88.23) |
| In-hospital delirium | 28 (71.79) | 15 (68.18) | 13 (76.47) |
| Pneumonia severity on admission | | | |
| Moderate, <i>n</i> (%) | 5 (12.82) | 2 (9.09) | 3 (17.64) |
| Serious, <i>n</i> (%) | 4 (10.25) | 1 (4.54) | 3 (17.64) |
| Severe, <i>n</i> (%) | 30 (76.92) | 19 (86.36) | 11 (64.7) |
| Oxygen therapy, <i>n</i> (%) | | | |
| Nasal cannula | 1 (2.56) | 1 (4.54) | 0 (0) |
| High-flow nasal cannula | 10 (25.64) | 5 (22.72) | 5 (29.41) |
| IMV | 28 (71.79) | 16 (72.72) | 12 (70.58) |
| Duration of IMV, <i>mean</i> (\pm <i>SD</i>) | 19.75 (\pm 22.29) | 23.81 (\pm 28.88) | 14.33 (\pm 5.19) |

Demographic data and symptoms reported at hospital admission for the whole sample and for the clustered groups based on cortical thickness atrophy. For each variable, we indicate the format of the values

IMV Invasive mechanical ventilation

wave of infections. Images were acquired using a Siemens Skyra 3 T MRI system at the INNN's MRI unit. T1-weighted 3D MPRAGE images were obtained with a TR of 2.2 ms, TE of 2.45 ms, slice thickness of 1 mm, no gap between slices, matrix size of 256 × 256, and voxel size of 1 mm × 1 mm × 1 mm.

Cortical thickness quantification

Each T1-weighted image was analyzed using Volbrain [33] (<https://volbrain.upv.es>) through two distinct pipelines, both aimed at determining cortical thickness: (1) Vol2brain [34], automates the brain segmentation into 135 regions of interest (ROI) and (2) CERES [35], focuses on cerebellar tissue segmentation, discerning 26 bilateral distinct structures, including lobules I–II, III, IV, V, VI, Crus I, Crus II, VIIB, VIIIA, VIIIB, IX, and X. Cortical thickness values are expressed in mm. Additionally, the total intracranial volume (TIV) was computed. Considering the potential confounding effect caused by TIV [36], a TIV correction was performed. Since

cortical thickness is a linear measure, the cubic root of TIV was calculated as a means to transform it from volumetric to unidimensional measurement, resulting in an adjusted TIV. Following this transformation, a linear regression model was implemented to correct the measurements of each structure, accounting for the adjusted TIV.

Cognitive assessment

Like the acquisition of magnetic resonance images, the cognitive evaluation was carried out at the INNN, between February 22 and June 15, 2021. Cognitive assessment encompassed various domains, including attention, visual and verbal memory, visuospatial functions, verbal naming, and executive functions. The evaluation involved the administration of the following tests: Montreal Cognitive Assessment (MoCA), Brief Attention Test (BAT), Rey-Osterrieth Complex Figure (copy and immediate recall), Hopkins Verbal Learning Test-Revised, Boston Naming Test, Digit Span Backward, Trail Making Test (TMT A and

B version), Stroop Test, and Verbal Fluency Tests (phonemic and semantic). To determine whether recovered patients displayed suboptimal performance in these tests, we utilized the formulas established for deriving normative data specific to neuropsychological assessments among Spanish speakers from Mexico [37]. These formulas enabled us to calculate z -scores, facilitating the subsequent identification of participants whose scores fell outside -1 standard deviation [38]. This criterion was employed to categorize recovered patients with low cognitive performance, providing a robust framework for comparison. It is important to note that these values are normative and should be viewed as a reference to assess the possibility of cognitive impairments.

Cluster analysis based on encephalic differences

Brain and cerebellar structures showing statistically significant differences between recovered patients and controls served as the foundation for investigating patterns of encephalic deterioration. Initially, the Hopkins statistic was calculated to assess cluster tendency. Following that, cluster stability and internal measures (connectivity, silhouette coefficient, and Dunn index) were conducted to compare clustering algorithms, and based on these results a hierarchical method was applied. Ward's minimum variance method was administered for computing the distance between clusters. Finally, the correlation between the cophenetic distances and the original distance data (dissimilarity information) was calculated. The cluster analysis was conducted using the statistical software R, version 2021.09.0 Build 351.

Principal component analysis

The biomarkers quantified during the in-hospital course of the disease included C-reactive protein, D-dimer, lactate dehydrogenase (LDH), fibrinogen, neutrophils, lymphocytes, platelets, and erythrocyte sedimentation rate (ESR). To enhance data interpretability and streamline the correlation analysis, we subjected the selected biochemical markers to principal component analysis (PCA) using MATLAB, version 2018b (MathWorks Inc., Natick, MA, USA). We extracted components with eigenvalues ≥ 1 and conducted a varimax rotation to optimize data visualization, resulting in orthogonal outcomes. The scores obtained for each component were converted into Z -scores for subsequent statistical analyses.

It is worth mentioning that a small subset of recovered patients had incomplete information in some of their clinical data (biomarkers). Due to the limited amount of missing data, data imputation was carried out for nine participants who had missing data to a certain extent (proportion of missing data available = 0.05). The data imputation process was executed using the Missing Data Imputation Toolbox (Folch-Fortuny et al., 2016), which was implemented in MATLAB.

Statistical analysis

For all datasets, standardized residuals were calculated, and the Shapiro–Wilk normality test was applied ($p < 0.05$). Cortical thickness comparisons were conducted between recovered patients and controls, and subsequently between Group 1 and Group 2 as identified through the clustering analysis of recovered patients. Depending on the normality of the data, either the t -test or the Mann–Whitney U -test was conducted. To account for the challenge of multiple comparisons, p -values were adjusted using the False Discovery Rate (FDR) method ($q = 0.05$). Additionally, effect sizes were computed using Cohen's d or r scores, as appropriate.

The biomarkers quantified on admission, organized by components following PCA analysis, were examined for correlations with cognitive performance scores and normalized cerebral and cerebellar cortical thickness regions. The choice between appropriate correlation coefficients, either the Pearson correlation coefficient or Spearman's Rho correlation, depended on the distribution characteristics of standardized residuals. Age and education were taken into account as covariates. To address multiple comparisons, the results were subjected to correction using the FDR method ($q = 0.05$). These analyses were conducted using R version R i386 3.6.0 and RStudio version 2021.09.0 Build 351.

Results

Neuroanatomical results

The analysis of cortical thickness between recovered COVID-19 patients and controls revealed significant structural differences across several cerebral and cerebellar regions. These included the frontal lobe: left medial frontal gyrus, right straight gyrus, right medial orbital gyrus, right medial segment of precentral gyrus, and right supplementary motor cortex. Additionally, differences were observed in the temporal lobe, specifically the right temporal pole; in the occipital lobe, affecting the left inferior occipital gyrus, left medial occipital gyrus, and left occipital pole; within the limbic area, encompassing the right limbic cortex, right entorhinal area, and right parahippocampal gyrus; and finally, across cerebellar lobes, involving bilateral lobes IV, V, VI, left lobes crus II, VIIB, VIIB, VIIB, VIIB, IX, and bilateral lobes X. It is important to note that for the left middle and inferior occipital gyrus, left occipital pole and lobes crus II to IX of the cerebellum, recovered patients exhibited greater cortical thickness compared to controls (Table 2). Note that a lower cortical thickness is observed in most of the areas, except in structures of the occipital lobe and some lobes of the cerebellum.

Table 2 COVID-19 recovered patients' structures with statistical differences against the control group

| | Control group ($n=39$, 13 females) | | Patients ($n=39$, 11 females) | | Statistic | p -value _{FDR} | Effect size |
|---------------------------------------|--------------------------------------|--------------|---------------------------------|--------------|-----------|---------------------------|-------------|
| | Mean \pm SD | Median (IQR) | Mean \pm SD | Median (IQR) | | | |
| Age at examination, mean \pm SD | 55.15 \pm 9.95 | | 55.80 \pm 9.34 | | -0.29 | 0.76 | -0.06 |
| Structure | Mean \pm SD | Median (IQR) | Mean \pm SD | Median (IQR) | | | |
| Middle frontal gyrus left | 2.17 \pm 0.35 | 2.09 (0.53) | 1.96 \pm 0.33 | 1.95 (0.44) | 2.66 | 0.04 | 0.60 |
| Gyrus rectus left | 3.09 \pm 0.39 | 3.09 (0.54) | 2.82 \pm 0.49 | 2.71 (0.49) | 1058 | 0.01 | 0.33 |
| Medial orbital gyrus right | 2.97 \pm 0.39 | 2.90 (0.51) | 2.72 \pm 0.37 | 2.68 (0.42) | 107 | 0.01 | 0.35 |
| Precentral gyrus medial segment right | 1.72 \pm 0.32 | 1.69 (0.45) | 1.52 \pm 0.29 | 1.55 (0.42) | 1037 | 0.03 | 0.31 |
| Supplementary motor cortex right | 2.34 \pm 0.32 | 2.26 (0.49) | 2.07 \pm 0.32 | 2.03 (0.50) | 3.72 | <0.01 | 0.84 |
| Temporal pole right | 3.54 \pm 0.32 | 3.56 (0.37) | 3.29 \pm 0.40 | 3.27 (0.46) | 3.05 | 0.01 | 0.69 |
| Inferior occipital gyrus left | 2.23 \pm 0.32 | 2.19 (0.41) | 2.42 \pm 0.29 | 2.39 (0.40) | -2.92 | 0.02 | -0.66 |
| Middle occipital gyrus left | 2.38 \pm 0.36 | 2.34 (0.49) | 2.60 \pm 0.39 | 2.61 (0.51) | -2.65 | 0.04 | -0.60 |
| Occipital pole left | 1.16 \pm 0.31 | 1.11 (0.37) | 1.42 \pm 0.40 | 1.33 (0.64) | 441 | 0.012 | 0.36 |
| Limbic cortex right | 3.11 \pm 0.21 | 3.10 (0.27) | 2.92 \pm 0.28 | 2.93 (0.36) | 3.31 | 0.01 | 0.75 |
| Entorhinal area right | 3.43 \pm 0.22 | 3.48 (0.28) | 3.28 \pm 0.22 | 3.31 (0.38) | 3.06 | 0.01 | 0.69 |
| Parahippocampal gyrus right | 2.76 \pm 0.29 | 2.73 (0.30) | 2.59 \pm 0.22 | 2.57 (0.34) | 3.08 | 0.01 | 0.69 |
| Lobule IV left | 4.94 \pm 0.15 | 4.95 (0.21) | 4.81 \pm 0.19 | 4.85 (0.27) | 3.55 | <0.01 | 0.80 |
| Lobule IV right | 4.85 \pm 0.21 | 4.86 (0.27) | 4.63 \pm 0.23 | 4.65 (0.42) | 4.27 | <0.01 | 0.96 |
| Lobule V right | 4.77 \pm 0.26 | 4.76 (0.34) | 4.45 \pm 0.25 | 4.44 (0.36) | 5.45 | <0.01 | 1.23 |
| Lobule V left | 4.93 \pm 0.19 | 4.97 (0.28) | 4.75 \pm 0.20 | 4.77 (0.18) | 1164 | <0.01 | 0.45 |
| Lobule VI left | 4.79 \pm 0.26 | 4.77 (0.33) | 4.59 \pm 0.19 | 4.63 (0.28) | 1108 | <0.01 | 0.39 |
| Lobule VI right | 4.72 \pm 0.30 | 4.75 (0.48) | 4.29 \pm 0.29 | 4.33 (0.36) | 1.280 | <0.01 | 0.58 |
| Lobule Crus II left | 4.32 \pm 0.41 | 4.41 (0.53) | 4.58 \pm 0.19 | 4.61 (0.21) | 453 | 0.01 | 0.34 |
| Lobule VIIIB left | 4.70 \pm 0.27 | 4.72 (0.30) | 4.91 \pm 0.13 | 4.89 (0.20) | 363 | <0.01 | 0.45 |
| Lobule VIIIB left | 4.88 \pm 0.21 | 4.94 (0.33) | 5.05 \pm 0.13 | 5.06 (0.20) | 405 | <0.01 | 0.40 |
| Lobule VIIIA left | 4.83 \pm 0.17 | 4.85 (0.21) | 5.00 \pm 0.14 | 4.99 (0.21) | -5.01 | <0.01 | -1.14 |
| Lobule IX left | 3.76 \pm 0.39 | 3.75 (0.61) | 4.00 \pm 0.29 | 3.99 (0.36) | -3.16 | 0.01 | -0.71 |
| Lobule X left | 2.81 \pm 0.41 | 2.87 (0.58) | 2.30 \pm 0.42 | 2.29 (0.59) | 5.74 | <0.01 | 1.30 |
| Lobule X right | 2.21 \pm 0.44 | 2.13 (0.74) | 1.96 \pm 0.32 | 1.91 (0.46) | 2.81 | 0.03 | 0.63 |

Patient and the control groups' cortical thickness evidencing global encephalic changes after T -student and Mann-Whitney U test

Recovered COVID-19 patients' clusterization and within-group comparison

Subsequently, the entire set of structures displaying differences in cortical thickness among recovered patients was examined to identify whether patients exhibited distinct profiles of structural differences. To confirm inherent clustering tendencies, the Hopkins statistic (H) was utilized, yielding a statistic indicating a tendency for cluster formation ($H=0.59$). As a result, hierarchical cluster analysis using the Ward method was applied, resulting in the formation of 2 groups. Likewise, cophenetic distances were computed, yielding a correlation coefficient of 0.55. The dendrogram classified recovered patients into Group 1 ($n=22$) and Group 2 ($n=17$) (Fig. 1).

Following the formation of these two groups, a comparative analysis was conducted between them. The results revealed statistically significant differences, in

that sense. Group 1 exhibited reduced cortical thickness in cerebral structures, including left middle frontal gyrus, right gyrus rectus, right medial orbital gyrus, and right supplementary motor cortex in the frontal lobe; the right temporal pole in the temporal lobe; the right limbic cortex, right entorhinal area, and right parahippocampal gyrus in the limbic area. In contrast, Group 2 displayed lower cortical thickness in the cerebellum, particularly in the left lobule VIIIA and left lobule VIIIB (Table 3).

Similarly, a comparative analysis was conducted to contrast the results of clinical and cognitive tests between the groups of recovered patients. However, no statistically significant differences were observed in terms of cognitive performance or biomarkers between the two groups of patients. Only D-dimer showed a tendency of differences intra-groups (D-dimer p -uncorrected = 0.03; p -adjusted = 0.10; $U = 251$; $r = 0.34$) (supplementary material).

Fig.1 Dendrogram showing the hierarchical cluster analysis. The y-axis of the dendrogram refers to the “height” which is the measure of the distance or similarity between the groups in the hierarchical clustering analysis. The x-axis represents the groups formed by the cluster analysis. Group 1 consists of 22 patients who presented less cerebral cortical thickness (shown in red). Group 2 comprises 17 patients who presented changes in cerebellar cortical thickness (shown in blue)

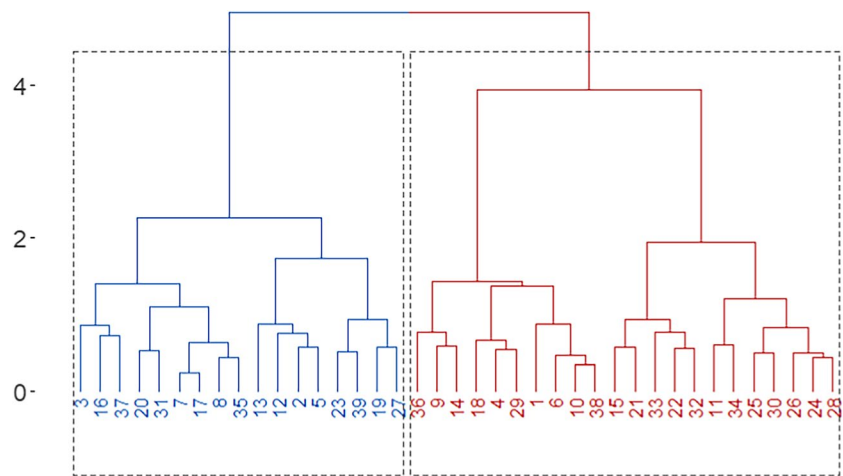


Table 3 Statistical significant differences between the groups formed by the cluster analysis

| | Group 1 (n=22, 5 females) | | Group 2 (n=17, 6 females) | | Statistic | p-value _{FDR} | Effect size |
|---|---------------------------|-----------------------|---------------------------|-----------------------|-----------|------------------------|-------------|
| Age at examination, <i>mean</i> ± <i>SD</i> | 57.93 ± 7.28 | | 53.05 ± 11.1 | | 1.65 | 0.10 | 0.51 |
| Education, <i>mean</i> ± <i>SD</i> | 11.63 ± 4.55 | | 11.23 ± 3.94 | | .289 | 0.77 | 0.09 |
| Structure | <i>Mean</i> ± <i>SD</i> | Median (<i>IQR</i>) | <i>Mean</i> ± <i>SD</i> | Median (<i>IQR</i>) | | | |
| Middle frontal gyrus left | 1.84 ± 0.27 | 1.87 (0.36) | 2.12 ± 0.36 | 2.09 (0.44) | -2.75 | 0.02 | -0.89 |
| Right gyrus rectus | 2.57 ± 0.35 | 2.55 (0.36) | 3.14 ± 0.47 | 2.94 (0.58) | -4.23 | <0.01 | -1.36 |
| Right medial orbital gyrus | 2.55 ± 0.20 | 2.58 (0.29) | 2.95 ± 0.40 | 2.81 (0.57) | -3.69 | <0.01 | -1.23 |
| Right supplementary motor cortex | 1.94 ± 0.24 | 1.91 (0.32) | 2.22 ± 0.35 | 2.27 (0.43) | -2.85 | 0.02 | -0.92 |
| Right temporal pole | 3.10 ± 0.35 | 3.14 (0.36) | 3.53 ± 0.33 | 3.43 (0.42) | -3.88 | <0.01 | -1.25 |
| Right entorhinal area | 3.18 ± 0.19 | 3.22 (0.28) | 3.41 ± 0.20 | 3.41 (0.23) | -3.58 | <0.01 | -1.15 |
| Right limbic cortex | 2.78 ± 0.22 | 2.79 (0.29) | 3.12 ± 0.23 | 3.09 (0.20) | -4.62 | <0.01 | -1.49 |
| Right parahippocampal gyrus | 2.51 ± 0.20 | 2.4874 (0.23) | 2.70 ± 0.18 | 2.72 (0.23) | -2.96 | 0.01 | -0.95 |
| Left VIIIA | 5.05 ± 0.14 | 5.06 (0.20) | 4.94 ± 0.08 | 4.93 (0.14) | 2.65 | 0.02 | 0.85 |
| Left VIIIB | 5.10 ± 0.09 | 5.09 (0.16) | 4.99 ± 0.12 | 4.98 (0.18) | 3.00 | 0.01 | 0.96 |

Values (mm) of encephalic structures that were different between group 1 and group 2

Clinical biochemical data

The clinical biochemical data including blood biochemistry, inflammatory markers, and coagulation factor measurements were obtained at the beginning of hospitalization (Table 4). It is important to note the subtle differences in the immune response, thrombotic and inflammatory features, and their association with each cluster.

Cognitive results

On the other hand, normative data proposed for the Mexican population were utilized as a reference to determine poor cognitive performance. Recovered patients who achieved scores > -1 standard deviation were selected to represent the percentage of patients who could indicate potentially poor performance compared to normative data (Table 5).

Principal component analysis

The PCA analysis of the biomarkers revealed that the first three components accounted for 69.17% of the total variance. These obtained components aligned with previously published findings [39]. Each component was assigned a distinct label: *PC1* = thromboinflammation (IL-6): C-reactive protein, fibrinogen, and lymphocytes (34.46% of variance). *PC2* = myeloid lineage: neutrophils, platelets, and ESR (19.97% of variance). *PC3* = systemic inflammation: D-dimer and lactate dehydrogenase (LDH) (14.73% of variance). Furthermore, an analysis was conducted to investigate whether there were differences among these components within the recovered patient groups. However, the analysis did not reveal statistically significant disparities across these components within the recovered patient groups (*PC1*: $p=0.3$; *PC2*: $p=0.4$; *PC3*: $p=0.5$).

Table 4 COVID-19 patients' clinical features on admission and their subsequent grouping after hierarchical cluster analysis

| | All patients | Cluster analysis of Cortical thickness | |
|---|------------------------|--|------------------------|
| | | Group 1 | Group 2 |
| Blood workup on admission, <i>mean</i> (\pm <i>SD</i>) | | | |
| Leucocytes ($\times 10^9/L$) | 10.82 (\pm 5.07) | 11.19 (\pm 5.35) | 10.35 (\pm 4.82) |
| Neutrophil (%) | 85.08 (\pm 10.93) | 86 (\pm 10.98) | 83.96 (\pm 11.09) |
| Lymphocytes (%) | 9.92 (\pm 8.41) | 9.52 (8.18) | 10.4 (\pm 8.9) |
| Monocytes (%) | 4.49 (\pm 3.07) | 4.18 (\pm 3.34) | 4.88 (\pm 2.77) |
| Eosinophils (%) | 0.28 (\pm 0.99) | 0.14 (\pm 0.32) | 0.45 (\pm 1.44) |
| Basophils (%) | 0.2 (\pm 0.21) | 0.11 (\pm 0.1) | 0.3 (\pm 0.27) |
| Hemoglobin (g/dL) | 15.33 (\pm 1.72) | 15.5 (\pm 1.78) | 15.11 (\pm 1.68) |
| Platelets ($\times 10^9/L$) | 182.92 (\pm 144.54) | 170.09 (\pm 162.36) | 198.76 (\pm 121.98) |
| Inflammatory markers on hospital admission, <i>mean</i> (\pm <i>SD</i>) | | | |
| Creatinine (mg/dL) (<i>n</i> = 38, Group 1 = 21) | 0.65 (\pm 0.53) | 0.68 (\pm 0.61) | 0.62 (\pm 0.42) |
| Creatine phosphokinase (IU/L) (<i>n</i> = 37, Group 1 = 21) | 141.72 (\pm 183.74) | 108.04 (\pm 96.51) | 185.87 (\pm 253.83) |
| LDH (U/L) (<i>n</i> = 37, Group 1 = 21) | 475.94 (\pm 179.31) | 490.61 (\pm 183.02) | 456.68 (\pm 178.34) |
| CRP (mg/L) (<i>n</i> = 36, Group 1 = 20) | 17.48 (\pm 7.62) | 17.23 (\pm 6.71) | 17.79 (\pm 8.85) |
| D dimer (μ g/mL) (<i>n</i> = 36, Group 1 = 20) | 1.24 (\pm 1.47) | 1.55 (\pm 1.82) | 0.84 (\pm 0.74) |
| Fibrinogen (mg/dL) (<i>n</i> = 34, Group 1 = 20) | 746.61 (\pm 140.14) | 766.5 (\pm 133.25) | 718.21 (\pm 149.77) |
| ESR (mm/h) (<i>n</i> = 29, Group 1 = 17) | 28.51 (\pm 8.49) | 27.17 (\pm 10.51) | 30.41 (\pm 4.03) |
| Coagulation factor on hospital admission, <i>mean</i> (\pm <i>SD</i>) | | | |
| PT (s) (<i>n</i> = 34, Group 1 = 20) | 15.54 (\pm 5.52) | 14.81 (\pm 1.17) | 16.6 (\pm 8.56) |
| INR (<i>n</i> = 34, Group 1 = 20) | 1.09 (\pm 0.4) | 1.03 (\pm 0.08) | 1.16 (\pm 0.62) |
| aPTT (s) (<i>n</i> = 34, Group 1 = 20) | 41.71 (\pm 11.01) | 40.74 (\pm 5.94) | 43.10 (\pm 15.89) |

COVID-19 patient's biochemical features on admission and their subsequent grouping after cluster analysis

LDH lactate dehydrogenase. *CRP* C reactive protein. *ESR* erythrocyte sedimentation rate. *PT* prothrombin time. *INR* international normalized ratio. *aPTT* activated partial thromboplastin time

Correlations between cerebral-cerebellar cortical thickness and clinical biochemical data and cognitive performance

Correlation analysis was conducted between the PCA components 1–3 and the cerebral and cerebellar structures that exhibited differences between recovered patients and controls. Initially, a correlation analysis encompassed components 1–3 and all structures that had demonstrated disparities between recovered patients and controls. Subsequently, only those structures exhibiting reduced cortical thickness were chosen, and depending on whether they belonged to Group 1 or Group 2, they were correlated once more with the obtained components. Although no significant correlations were identified after adjusting the *p*-values, a discernible trend was observed, linking specific structures with thromboinflammation (*PC1* component) (Fig. 2).

On the other hand, in the correlation analysis between the affected structures and the cognitive tests, we initially considered the entire group of recovered patients, correlating cognitive scores with all the structures that had exhibited differences between recovered patients and controls. Subsequently, the analysis was conducted for specific groups

obtained from the cluster analysis. However, no statistically significant correlations were identified for either after *p*-value correction, although some correlation trends can be observed (see Supplementary Material).

Discussion

COVID-19 is a disease known to have neurological consequences, leading to changes in the gray matter of the brain, particularly evident in the reduction of cortical thickness [28, 29]. Here, we tested if it is possible to find an encephalic lesion pattern associated with this disease. Our study unveiled significant differences in cortical thickness between recovered COVID-19 patients and control subjects, with the most pronounced changes observed in the frontal and cerebellar regions, followed by lesions of the occipital and temporal lobes, as well as the limbic area.

Various authors have attempted to categorize the clinical profiles of COVID-19 patients. Some have identified distinct clinical phenotypes characterized by elevated levels of hypoxemia and their correlation with laboratory findings such as neutrophil and lymphocyte counts [40].

Table 5 Cognitive scores of COVID-19 recovered patients with cognitive impairment and their subsequent grouping after hierarchical cluster analysis

| Cognitive scores | Cluster analysis of cortical thickness | | | | | |
|--|--|------------|--------------------------|-----------|--------------------------|------------|
| | All patients (<i>n</i> = 39) | | Group 1 (<i>n</i> = 22) | | Group 2 (<i>n</i> = 17) | |
| <i>Mean of crude values (SD) / n (%)</i> | | | | | | |
| Montreal Cognitive Assessment (MoCA) | 25.94 (3.29) | 18 (46.15) | 26.13 (3.77) | 8 (36.36) | 25.70 (2.64) | 10 (58.82) |
| Boston Test | 50.69 (5.45) | 2 (5.12) | 51.40 (5.08) | 0 (0) | 49.76 (5.92) | 2 (11.11) |
| Verbal Fluency (F) | 11.76 (4.03) | 6 (15.38) | 12.18 (3.89) | 3 (13.63) | 11.23 (4.26) | 3 (16.66) |
| Verbal Fluency (A) | 9.9 (3.47) | 10 (25.64) | 9.09 (2.58) | 7 (31.81) | 11.11 (4.18) | 3 (16.66) |
| Verbal Fluency (S) | 10.69 (2.72) | 5 (12.82) | 10.63 (2.46) | 3 (13.63) | 10.76 (3.11) | 2 (11.11) |
| Verbal Fluency (animals) | 20.69 (3.95) | 1 (2.56) | 20.63 (4.38) | 1 (4.54) | 20.76 (3.45) | 0 (0) |
| Stroop Test | 31.87 (9.42) | 9 (23.07) | 32.77 (10.60) | 5 (22.72) | 30.70 (7.80) | 4 (23.52) |
| Digit Span (backward) | 3.56 (1.07) | 13 (33.33) | 3.77 (0.97) | 6 (27.27) | 3.29 (1.15) | 7 (41.17) |
| Trail Making Test Form A (TMT A) | 67.15 (24.79) | 11 (28.20) | 71.27 (28.66) | 7 (31.81) | 61.82 (18.10) | 4 (23.52) |
| Trail Making Test Form B (TMT B) | 159.58 (82.36) | 11 (28.20) | 160.72 (93.37) | 7 (31.81) | 158.11 (68.29) | 4 (23.52) |
| Hopkins Verbal Learning Test (sum of total trials) | 20.38 (4.22) | 3 (7.69) | 20.63 (4.81) | 2 (9.09) | 20.05 (3.41) | 1 (5.88) |
| Hopkins Verbal Learning Test (delayed recall) | 7.36 (2.24) | 3 (7.69) | 7.22 (2.28) | 2 (9.09) | 7.52 (2.23) | 1 (5.88) |
| Brief Test of Attention | 15.53 (3.16) | 1 (2.56) | 15.81 (3.09) | 1 (4.54) | 15.17 (3.32) | 0 (0) |
| Rey–Osterrieth Complex Figure (copy) | 32.52 (4.40) | 2 (5.12) | 32.43 (3.81) | 1 (4.54) | 32.64 (5.18) | 1 (5.88) |
| Rey–Osterrieth Complex Figure (recall) | 19.52 (6.50) | 4 (10.25) | 19.86 (6.01) | 1 (4.54) | 19.08 (7.25) | 3 (16.66) |

The first column of each group displays the mean raw score obtained in each cognitive test alongside its standard deviation. The second column indicates the number and percentage of patients who scored > -1 SD in comparison to the total number of patients ($n=39$). Subsequent columns present the count and percentage of patients within each group formed after cluster analysis

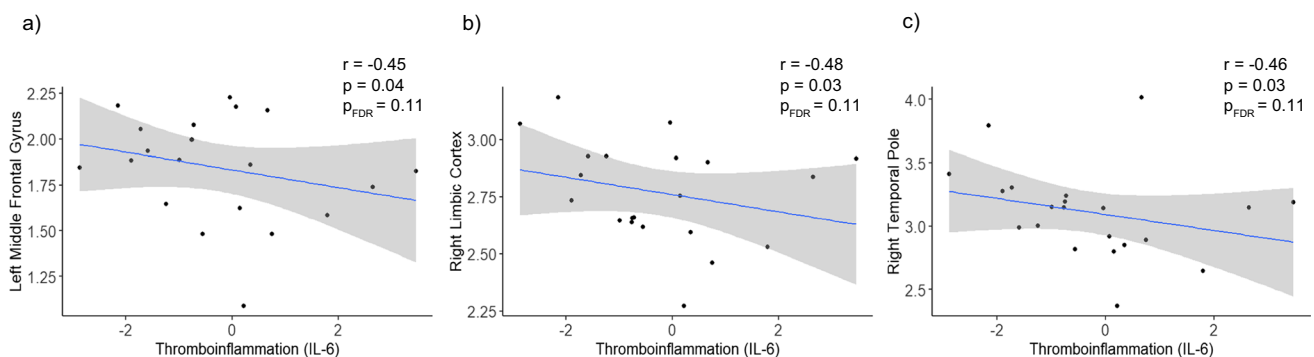


Fig. 2 Correlations between PC1 = thromboinflammation (IL-6) and cerebral structures. The brain structures that were significantly different between group 1 and group 2 and their association with thrombo-

inflammatory CP1 (IL6) are shown. A trend can be observed between the correlation of brain structures and said component

In our study, we opted to categorize patients based on the encephalic structures that displayed significant differences in cortical thickness between recovered COVID-19 patients and control subjects. This categorization resulted in two groups: one marked by reduced cortical thickness mainly in cerebral areas (Group 1) and the other characterized by changes with major impact in cerebellar areas (Group 2). This divergence in patterns may suggest two different mechanisms of viral involvement [41].

The existing literature presents several mechanisms through which SARS-CoV-2 can inflict damage on brain tissue [42]. These mechanisms encompass direct invasion via the olfactory nerve [11] or the vagus nerve [12], the formation of microthrombi [13–15], or alterations in blood–brain barrier permeability associated with neuroinflammation [16]. We hypothesized that these infection mechanisms might be linked to the distinct pattern observed in our study. Although there was no statistically significant difference between the patient

groups, a trend could be observed towards a higher incidence of dysgeusia and anosmia was more prevalent in Group 1 (as shown in Table 1). This observation holds significance as Group 1 is characterized by cerebral atrophy, suggesting that the olfactory nerve could serve as a potential route for viral entry into the central nervous system, thus contributing to the clinical manifestation of dysgeusia and anosmia. Additionally, despite both groups displaying a similar trend in terms of oxygen therapy, Group 1 had a longer average duration of mechanical ventilation [43].

The clinical-behavioral findings underscore a notable degree of uniformity within the recovered patient groups, particularly in terms of cognitive performance and the data derived from blood samples and inflammatory markers. Nevertheless, despite the absence of statistically significant differences in cognitive performance or clinical components after adjusting for *p*-values, a noticeable trend emerged concerning D-dimer levels. Group 1 exhibited higher values compared to Group 2. This observation lends support to the hypothesis of immunothrombosis as a potential mechanism of central nervous system damage [26, 44] with Group 1 displaying a more pronounced elevation. It prompts consideration of the possibility of additional ischemic damage associated with immunothrombosis, in addition to the direct entry of the virus into the brain. This process hinges not only on the state of inflammation in the brain but also on microthrombus formation and the ensuing tissue hypoxia it brings about. Prolonged periods of immobility [27, 45], a contributing factor to vascular stasis and a risk factor for thrombus formation, may exacerbate this process. D-dimer, in this context, serves as an indirect marker [46].

On the other hand, the predominance of cerebellar differences in Group 2 can be elucidated by considering three underlying factors. Firstly, the cerebellum houses a greater number of vascular structures that support peripheral circulation, making it a region less susceptible to ischemic processes [47]. However, this extensive vascularization comes with a double-edged nature; while it reduces susceptibility to ischemic injury, it also renders the region more responsive to inflammatory processes. This heightened sensitivity arises from inflammation being a process that involves both vascular and immune components [48]. Due to the greater vascularization in these regions, inflammatory processes can potentially induce more substantial local damage [49, 50]. Secondly, there exists a distinct pattern of immune expression within the central nervous system (CNS), where specific regions are more predisposed to heightened inflammatory responses and collateral damage to neural tissue [51, 52]. Thirdly, alterations in blood–brain barrier permeability can facilitate tissue damage through neuroinflammatory mechanisms and glial activation [17]. The convergence of these factors likely contributes to the observed preferential involvement of cerebellar structures in Group 2.

Moreover, it is noteworthy to highlight the observed increase in cortical thickness among patients in the occipital regions, suggesting a possible association with gliosis [53]. Prior research has indicated an increase in cortical thickness across different pathologies, which is thought to be linked to phenotypic alterations in glial cells during neuroinflammation, notably astrocytic soma hypertrophy [54–56]. However, it is crucial to acknowledge that further extensive investigation in future studies is necessary to elucidate the precise underlying mechanism driving this increased cortical thickness.

Lastly, concerning the cognitive aspect, it is crucial to emphasize that Group 1, which predominantly demonstrated cerebral damage, particularly in the frontal lobe [57] and medial temporal pole [58], exhibited a tendency to correlate with attention and working memory tasks. On the other hand, Group 2, which showed changes in the cerebellum, showed a correlation trend with visuospatial tasks (supplementary material). The role of the cerebellum in visuospatial functions has been previously studied [59, 60]. This observation underscores the intricate interplay between long-term structural damage and cognitive changes that depend on the pattern of atrophy exhibited in recovered COVID-19 patients.

The in-hospital course plays a fundamental role in the clinical presentations of recovered COVID-19 patients. Although our study contributes to the understanding of the causal factors underlying brain damage, subsequent studies should further consider other significant factors related to the evolution of COVID-19, including SARS-CoV-2 variations [61], the impact of vaccination, and the administration of therapeutic agents such as Paxlovid [62] and steroids in hospitalized patients [63]. These variables have the potential to influence disease progression and the development of sequelae. Therefore, appropriate clinical follow-up will enable timely support for patients experiencing sequelae.

Conclusions

Our results contribute valuable insights into the relationship between COVID-19 and encephalic structural alterations. Although this study is exploratory, it has revealed significant trends that can lay the groundwork for future research. In the first place, it was possible to characterize the integrity of the cerebral and cerebellar regions after the cluster analysis, observing the division of two groups, one with differences mainly in the brain and the other with changes in the cerebellum, this opens the possibility to speculate about the existence of different viral mechanisms of action that affect the CNS distinctly. Similarly, the results suggested a possible impact of inflammatory markers on the brain integrity in patients recovered from COVID-19. Future research

endeavors with larger sample sizes and additional comprehensive data collection would undoubtedly enhance the robustness of our findings, providing a better understanding of the long-term COVID-19 sequelae.

Limitations

We acknowledge that the present study may have certain limitations, with the most prominent being the relatively small sample size. This limitation may affect the generalizability of our findings to a broader population. Additionally, the absence of extensive and domain-specific cognitive assessments and comprehensive clinical data for the control group hampers the comparisons between this group and the recovered patient cohort, as well as the lack of cognitive evaluations prior to SARS-CoV-2 infection of patients. Furthermore, the unavailability of initial MRI scans upon hospitalization limited our capacity to conduct a comprehensive longitudinal analysis during the acute phase. Such an analysis would have offered valuable insights into the evolution of structural changes over time. Finally, given the specific nature of this cross-sectional study, it is important to note that the impact of COVID-19 variants, vaccination, and therapeutic interventions on disease progression and sequelae were not considered, as previously explained in the “[Participants](#)” section.

Code availability

Not applicable.

Supplementary Information The online version contains supplementary material available at <https://doi.org/10.1007/s10072-023-07266-x>.

Author contribution All the authors contributed to the study conception and design. Material preparation, data collection, and analysis were performed by all the authors. The first draft of the manuscript was written by Angel Omar Romero-Molina, and all the authors commented on the previous versions of the manuscript. All the authors read and approved the final manuscript.

Funding This work received funding from CONAHCYT–Mexico grant no. A1-S-10669 and PAPIIT-UNAM grant no. IN214122 given to Juan Fernandez-Ruiz and CONAHCYT–Mexico Ph.D. fellowship no. 789431 given to Angel Omar Romero Molina (CVU: 782944).

Data availability All the data supporting our findings are contained within the manuscript. De-identified data to replicate our results will be available to qualified researchers upon written request to the corresponding author.

Declarations Ethical approval and consent to participate

This project was approved by the research and ethical committee of the Instituto Nacional de Enfermedades Respiratorias under approval number C48-20 and the Instituto Nacional de Neurología y Neurocirugía under approval number 06–21. Signed informed consent was obtained

from all participants and the procedures about human research were according to the Helsinki declaration.

Conflict of interest The authors declare no competing interests.

Disclaimer The funders had no role in the study design, data collection and analysis, decision to publish, or preparation of the manuscript.

References

- Hu B, Guo H, Zhou P, Shi Z-L (2021) Characteristics of SARS-CoV-2 and COVID-19. *Nat Rev Microbiol* 19:141–154. <https://doi.org/10.1038/s41579-020-00459-7>
- Elrobaa IH, New KJ (2021) COVID-19: pulmonary and extra pulmonary manifestations. *Front Public Health* 9:711616. <https://doi.org/10.3389/fpubh.2021.711616>
- Shen Q, Li J, Zhang Z, Guo S, Wang Q, An X, Chang H (2022) COVID-19: systemic pathology and its implications for therapy. *Int J Biol Sci* 18:386–408. <https://doi.org/10.7150/ijbs.65911>
- Al-Sarraj S, Troakes C, Hanley B, Osborn M, Richardson MP, Hotopf M, Bullmore E, Everall IP (2021) Invited review: the spectrum of neuropathology in COVID-19. *Neuropathol Appl Neurobiol* 47:3–16. <https://doi.org/10.1111/nan.12667>
- Di Carlo DT, Montemurro N, Petrella G, Siciliano G, Ceravolo R, Perrini P (2021) Exploring the clinical association between neurological symptoms and COVID-19 pandemic outbreak: a systematic review of current literature. *J Neurol* 268:1561–1569. <https://doi.org/10.1007/s00415-020-09978-y>
- Docherty AB, Harrison EM, Green CA, Hardwick HE, Pius R, Norman L, Holden KA, Read JM, Dondelinger F, Carson G, Merson L, Lee J, Plotkin D, Sigfrid L, Halpin S, Jackson C, Gamble C, Horby PW, Nguyen-Van-Tam JS, Ho A, Russell CD, Dunning J, Openshaw PJ, Baillie JK, Semples MG (2020) Features of 20 133 UK patients in hospital with COVID-19 using the ISARIC WHO clinical characterisation protocol: prospective observational cohort study. *BMJ* 369:m1985. <https://doi.org/10.1136/bmj.m1985>
- Mao L, Jin H, Wang M, Hu Y, Chen S, He Q, Chang J, Hong C, Zhou Y, Wang D, Miao X, Li Y, Hu B (2020) Neurologic manifestations of hospitalized patients with coronavirus disease 2019 in Wuhan. *China JAMA Neurol* 77:683. <https://doi.org/10.1001/jamaneurol.2020.1127>
- Ferrucci R, Dini M, Groppo E, Rosci C, Reitano MR, Bai F, Poletti B, Brugnera A, Silani V, D’Arminio Monforte A, Priori A (2021) Long-lasting cognitive abnormalities after COVID-19. *Brain Sci* 11:235. <https://doi.org/10.3390/brainsci11020235>
- Mendelson M, Nel J, Blumberg L, Madhi SA, Dryden M, Stevens W, Venter FWD (2021) Long-COVID: an evolving problem with an extensive impact. *S Afr Med J* 111:10–12. <https://doi.org/10.7196/SAMJ.2021.v111i1.15433>
- Mishra SS, Hafiz R, Misra R, Gandhi TK, Prasad A, Mahajan V, Biswal BB (2022) Brain Alterations in COVID recovered revealed by susceptibility-weighted magnetic resonance imaging. <https://doi.org/10.1101/2022.11.21.22282600>
- Kumar M, Thakur AK (2020) Neurological manifestations and comorbidity associated with COVID-19: an overview. *Neurol Sci* 41:3409–3418. <https://doi.org/10.1007/s10072-020-04823-6>
- Woo MS, Shafiq M, Fitzek A, Dottermusch M, Altmeppen H, Mohammadi B, Mayer C, Bal LC, Raich L, Matschke J, Krusemann S, Pfeifferle S, Brehm TT, Lütgehetmann M, Schädler J, Addo MM, Schulze zur Wiesch J, Ondruschka B, Friese MA, Glatzel M, (2023) Vagus nerve inflammation contributes to

- dysautonomia in COVID-19. *Acta Neuropathol (Berl)* 146:387–394. <https://doi.org/10.1007/s00401-023-02612-x>
13. Cacciola R, GentiliniCacciola E, Vecchio V, Cacciola E (2022) Cellular and molecular mechanisms in COVID-19 coagulopathy: role of inflammation and endotheliopathy. *J Thromb Thrombolysis* 53:282–290. <https://doi.org/10.1007/s11239-021-02583-4>
 14. Pretorius E, Venter C, Laubscher GJ, Kotze MJ, Oladejo SO, Watson LR, Rajaratnam K, Watson BW, Kell DB (2022) Prevalence of symptoms, comorbidities, fibrin amyloid microclots and platelet pathology in individuals with long COVID/post-acute sequelae of COVID-19 (PASC). *Cardiovasc Diabetol* 21:148. <https://doi.org/10.1186/s12933-022-01579-5>
 15. Fogarty H, Townsend L, Morrin H, Ahmad A, Comerford C, Karampini E, Englert H, Byrne M, Bergin C, O'Sullivan JM, Martin-Loeches I, Nadarajan P, Bannan C, Mallon PW, Curley GF, Preston RJS, Rehill AM, McGonagle D, Ni Cheallaigh C, Baker RI, Renné T, Ward SE, O'Donnell JS, Investigators the IC-19 VS (iCVS) (2021) Persistent endotheliopathy in the pathogenesis of long COVID syndrome. *J Thromb Haemost* 19:2546–2553. <https://doi.org/10.1111/jth.15490>
 16. Wan D, Du T, Hong W, Chen L, Que H, Lu S, Peng X (2021) Neurological complications and infection mechanism of SARS-CoV-2. *Signal Transduct Target Ther* 6:406. <https://doi.org/10.1038/s41392-021-00818-7>
 17. Vanderheiden A, Klein RS (2022) Neuroinflammation and COVID-19. *Curr Opin Neurobiol* 76:102608. <https://doi.org/10.1016/j.conb.2022.102608>
 18. Besteher B, Machnik M, Troll M, Toepffer A, Zerekidze A, Rocktäschel T, Heller C, Kikinis Z, Brodoehl S, Finke K, Reuken PA, Opel N, Stallmach A, Gaser C, Walter M (2022) Larger gray matter volumes in neuropsychiatric long-COVID syndrome. *Psychiatry Res* 317:114836. <https://doi.org/10.1016/j.psychres.2022.114836>
 19. Tremblay M-E, Madore C, Bordeleau M, Tian L, Verkhatsky A (2020) Neuropathobiology of COVID-19: the role for glia. *Front Cell Neurosci* 14:1–15. <https://doi.org/10.3389/fncel.2020.592214>
 20. Tsagkaris C, Bilal M, Aktar I, Aboufandi Y, Tas A, Aborode AT, Suvvari TK, Ahmad S, Shkodina A, Phadke R, Emhamed MS, Baig AA, Alexiou A, Ashraf GMd, Kamal MA (2022) Cytokine storm and neuropathological alterations in patients with neurological manifestations of COVID-19. *Curr Alzheimer Res* 19:641–657. <https://doi.org/10.2174/1567205019666220908084559>
 21. Qin C, Zhou L, Hu Z, Zhang S, Yang S, Tao Y, Xie C, Ma K, Shang K, Wang W, Tian D-S (2020) Dysregulation of immune response in patients with coronavirus 2019 (COVID-19) in Wuhan, China. *Clin Infect Dis* 71:762–768. <https://doi.org/10.1093/cid/ciaa248>
 22. Hong L-Z, Shou Z-X, Zheng D-M, Jin X (2021) The most important biomarker associated with coagulation and inflammation among COVID-19 patients. *Mol Cell Biochem* 476:2877–2885. <https://doi.org/10.1007/s11010-021-04122-4>
 23. Lai Y-J, Liu S-H, Manachevakul S, Lee T-A, Kuo C-T, Bello D (2023) Biomarkers in long COVID-19: a systematic review. *Front Med* 10:1–10. <https://doi.org/10.3389/fmed.2023.1085988>
 24. Coomes EA, Haghbayan H (2020) Interleukin-6 in Covid-19: a systematic review and meta-analysis. *Rev Med Virol* 30:e2141. <https://doi.org/10.1002/rmv.2141>
 25. Gu SX, Tyagi T, Jain K, Gu VW, Lee SH, Hwa JM, Kwan JM, Krause DS, Lee AI, Halene S, Martin KA, Chun HJ, Hwa J (2021) Thrombocytopeny and endotheliopathy: crucial contributors to COVID-19 thromboinflammation. *Nat Rev Cardiol* 18:194–209. <https://doi.org/10.1038/s41569-020-00469-1>
 26. Bonaventura A, Vecchié A, Dagna L, Martinod K, Dixon DL, Van Tassel BW, Dentali F, Montecucco F, Massberg S, Levi M, Abbate A (2021) Endothelial dysfunction and immunothrombosis as key pathogenic mechanisms in COVID-19. *Nat Rev Immunol* 21:319–329. <https://doi.org/10.1038/s41577-021-00536-9>
 27. Townsend L, Fogarty H, Dyer A, Martin-Loeches I, Bannan C, Nadarajan P, Bergin C, O'Farrelly C, Conlon N, Bourke NM, Ward SE, Byrne M, Ryan K, O'Connell N, O'Sullivan JM, Ni Cheallaigh C, O'Donnell JS (2021) Prolonged elevation of D-dimer levels in convalescent COVID-19 patients is independent of the acute phase response. *J Thromb Haemost* 19:1064–1070. <https://doi.org/10.1111/jth.15267>
 28. Lu Y, Li X, Geng D, Mei N, Wu P-Y, Huang C-C, Jia T, Zhao Y, Wang D, Xiao A, Yin B (2020) Cerebral micro-structural changes in COVID-19 patients – an MRI-based 3-month follow-up study. *eClinicalMedicine* 25. <https://doi.org/10.1016/j.eclinm.2020.100484>
 29. Douaud G, Lee S, Alfaro-Almagro F, Arthofer C, Wang C, McCarthy P, Lange F, Andersson JLR, Griffanti L, Duff E, Jbabdi S, Tschler B, Keating P, Winkler AM, Collins R, Matthews PM, Allen N, Miller KL, Nichols TE, Smith SM (2022) SARS-CoV-2 is associated with changes in brain structure in UK Biobank. *Nature* 604:697–707. <https://doi.org/10.1038/s41586-022-04569-5>
 30. Manca R, De Marco M, Ince PG, Venneri A (2021) Heterogeneity in regional damage detected by neuroimaging and neuropathological studies in older adults with COVID-19: a cognitive-neuroscience systematic review to inform the long-term impact of the virus on neurocognitive trajectories. *Front Aging Neurosci* 13:1–29. <https://doi.org/10.3389/fnagi.2021.646908>
 31. Díez-Cirarda M, Yus M, Gómez-Ruiz N, Polidura C, Gil-Martínez L, Delgado-Alonso C, Jorquera M, Gómez-Pinedo U, Matias-Guiu J, Arrazola J, Matias-Guiu JA (2023) Multimodal neuroimaging in post-COVID syndrome and correlation with cognition. *Brain* 146:2142–2152. <https://doi.org/10.1093/brain/awac384>
 32. Du Y, Zhao W, Huang S, Huang Y, Chen Y, Zhang H, Guo H, Liu J (2023) Two-year follow-up of brain structural changes in patients who recovered from COVID-19: a prospective study. *Psychiatry Res* 319:114969. <https://doi.org/10.1016/j.psychres.2022.114969>
 33. Manjón JV, Coupé P (2016) volBrain: an online MRI brain volumetry system. *Front Neuroinformatics* 10:1–14. <https://doi.org/10.3389/fninf.2016.00030>
 34. Manjón JV, Romero JE, Vivo-Hernando R, Rubio G, Aparici F, de la Iglesia-Vaya M, Coupé P (2022) vol2Brain: a new online pipeline for whole brain MRI analysis. *Front Neuroinformatics* 16:1–11. <https://doi.org/10.3389/fninf.2022.862805>
 35. Romero JE, Coupé P, Giraud R, Ta V-T, Fonov V, Park MTM, Chakravarty MM, Voineskos AN, Manjón JV (2017) CERES: a new cerebellum lobule segmentation method. *Neuroimage* 147:916–924. <https://doi.org/10.1016/j.neuroimage.2016.11.003>
 36. Sanchis-Segura C, Ibañez-Gual MV, Aguirre N, Cruz-Gómez AJ, Forn C (2020) Effects of different intracranial volume correction methods on univariate sex differences in grey matter volume and multivariate sex prediction. *Sci Rep* 10:12953. <https://doi.org/10.1038/s41598-020-69361-9>
 37. Guàrdia-Olmos J, Però-Cebollero M, Rivera D, Arango-Lasprilla JC (2015) Methodology for the development of normative data for ten Spanish-language neuropsychological tests in eleven Latin American countries. *NeuroRehabilitation* 37:493–499. <https://doi.org/10.3233/NRE-151277>
 38. Tedesco AM, Chiricozzi FR, Clausi S, Lupo M, Molinari M, Leggio MG (2011) The cerebellar cognitive profile. *Brain* 134:3672–3686. <https://doi.org/10.1093/brain/awr266>
 39. García-Grimshaw M, Chirino-Pérez A, Flores-Silva FD, Valdés-Ferrer SI, Vargas-Martínez M de los Á, Jiménez-Ávila AI, Chávez-Martínez OA, Ramos-Galicia EM, Marché-Fernández OA, Ramírez-Carrillo MF, Grajeda-González SL, Ramírez-Jiménez ME, Chávez-Manzanera EA, Tusié-Luna MT, Ochoa-Guzmán A, Cantú-Brito C, Fernandez-Ruiz J, Chiquete E (2022) Critical role of acute hypoxemia on the cognitive impairment after severe COVID-19 pneumonia: a multivariate causality model analysis. *Neurol Sci* 43:2217–2229. <https://doi.org/10.1007/s10072-021-05798-8>

40. Yamga E, Mullie L, Durand M, Cadrin-Chenevert A, Tang A, Montagnon E, Chartrand-Lefebvre C, Chassé M (2023) Interpretable clinical phenotypes among patients hospitalized with COVID-19 using cluster analysis. *Front Digit Health* 5:1–13. <https://doi.org/10.3389/fdgth.2023.1142822>
41. Bougakov D, Podell K, Goldberg E (2021) Multiple neuroinvasive pathways in COVID-19. *Mol Neurobiol* 58:564–575. <https://doi.org/10.1007/s12035-020-02152-5>
42. Aghagholi G, Gallo Marin B, Katchur NJ, Chaves-Sell F, Asaad WF, Murphy SA (2021) Neurological involvement in COVID-19 and potential mechanisms: a review. *Neurocrit Care* 34:1062–1071. <https://doi.org/10.1007/s12028-020-01049-4>
43. Meinhardt J, Radke J, Dittmayer C, Franz J, Thomas C, Mothes R, Laue M, Schneider J, Brünink S, Greuel S, Lehmann M, Hassan O, Aschman T, Schumann E, Chua RL, Conrad C, Eils R, Stenzel W, Windgassen M, Rößler L, Goebel H-H, Gelderblom HR, Martin H, Nitsche A, Schulz-Schaeffer WJ, Hakroush S, Winkler MS, Tampe B, Scheibe F, Körtvélyessy P, Reinhold D, Siegmund B, Kühl AA, Elezkurtaj S, Horst D, Oesterhelweg L, Tsokos M, Ingold-Heppner B, Stadelmann C, Drosten C, Corman VM, Radrbruch H, Heppner FL (2021) Olfactory transmucosal SARS-CoV-2 invasion as a port of central nervous system entry in individuals with COVID-19. *Nat Neurosci* 24:168–175. <https://doi.org/10.1038/s41593-020-00758-5>
44. Zhu Y, Chen X, Liu X (2022) NETosis and neutrophil extracellular traps in COVID-19: immunothrombosis and Beyond. *Front Immunol* 13:1–11. <https://doi.org/10.3389/fimmu.2022.838011>
45. Bivona G, Agnello L, Ciaccio M (2021) Biomarkers for prognosis and treatment response in COVID-19 patients. *Ann Lab Med* 41:540–548. <https://doi.org/10.3343/alm.2021.41.6.540>
46. Eljilany I, Elzouki A-N (2020) D-Dimer, Fibrinogen, and IL-6 in COVID-19 patients with suspected venous thromboembolism: a narrative review. *Vasc Health Risk Manag* 16:455–462. <https://doi.org/10.2147/VHRM.S280962>
47. Johnson MH, Christman CW (1995) Posterior circulation infarction: anatomy, pathophysiology, and clinical correlation. *Semin Ultrasound CT MRI* 16:237–252. [https://doi.org/10.1016/0887-2171\(95\)90020-9](https://doi.org/10.1016/0887-2171(95)90020-9)
48. Lentsch AB, Ward PA (2000) Regulation of inflammatory vascular damage. *J Pathol* 190:343–348. [https://doi.org/10.1002/\(SICI\)1096-9896\(200002\)190:3%3c343::AID-PATH522%3e3.0.CO;2-M](https://doi.org/10.1002/(SICI)1096-9896(200002)190:3%3c343::AID-PATH522%3e3.0.CO;2-M)
49. Parvez MSA, Ohtsuki G (2022) Acute cerebellar inflammation and related ataxia: mechanisms and pathophysiology. *Brain Sci* 12:367. <https://doi.org/10.3390/brainsci12030367>
50. Sawaishi Y, Takada G (2002) Acute cerebellitis. *The Cerebellum* 1:223–228. <https://doi.org/10.1080/14734220260418457>
51. Kipp M, Norkute A, Johann S, Lorenz L, Braun A, Hieble A, Gingele S, Pott F, Richter J, Beyer C (2008) Brain-region-specific astroglial responses in vitro after LPS exposure. *J Mol Neurosci* 35:235–243. <https://doi.org/10.1007/s12031-008-9057-7>
52. Shastri A, Bonifati DM, Kishore U (2013) Innate immunity and neuroinflammation. *Mediators Inflamm* 2013:1–19. <https://doi.org/10.1155/2013/342931>
53. Escartin C, Guillemaud O, Carrillo-de Sauvage M-A (2019) Questions and (some) answers on reactive astrocytes. *Glia* 67:2221–2247. <https://doi.org/10.1002/glia.23687>
54. Kang K, Han J, Lee S-W, Jeong SY, Lim Y-H, Lee J-M, Yoon U (2020) Abnormal cortical thickening and thinning in idiopathic normal-pressure hydrocephalus. *Sci Rep* 10:21213. <https://doi.org/10.1038/s41598-020-78067-x>
55. Zimmermann N, Goulart Corrêa D, Tukamoto G, Netto T, Batista Pereira D, Paz Fonseca R, Gasparetto EL (2017) Brain morphology and cortical thickness variations in systemic lupus erythematosus patients: differences among neurological, psychiatric, and nonneuropsychiatric manifestations. *J Magn Reson Imaging* 46:150–158. <https://doi.org/10.1002/jmri.25538>
56. Batzu L, Westman E, Pereira JB (2020) Cerebrospinal fluid progranulin is associated with increased cortical thickness in early stages of Alzheimer's disease. *Neurobiol Aging* 88:61–70. <https://doi.org/10.1016/j.neurobiolaging.2019.12.012>
57. Alvarez JA, Emory E (2006) Executive function and the frontal lobes: a meta-analytic review. *Neuropsychol Rev* 16:17–42. <https://doi.org/10.1007/s11065-006-9002-x>
58. Herlin B, Navarro V, Dupont S (2021) The temporal pole: from anatomy to function—a literature appraisal. *J Chem Neuroanat* 113:101925. <https://doi.org/10.1016/j.jchemneu.2021.101925>
59. Baillieux H, Smet HJD, Paquier PF, De Deyn PP, Mariën P (2008) Cerebellar neurocognition: insights into the bottom of the brain. *Clin Neurol Neurosurg* 110:763–773. <https://doi.org/10.1016/j.clineuro.2008.05.013>
60. Timmann D, Daum I (2007) Cerebellar contributions to cognitive functions: a progress report after two decades of research. *The Cerebellum* 6:159–162. <https://doi.org/10.1080/14734220701496448>
61. Maslo C, Friedland R, Toubkin M, Laubscher A, Akaloo T, Kama B (2022) Characteristics and outcomes of hospitalized patients in South Africa during the COVID-19 omicron wave compared with previous waves. *JAMA* 327:583–584. <https://doi.org/10.1001/jama.2021.24868>
62. Wen W, Chen C, Tang J, Wang C, Zhou M, Cheng Y, Zhou X, Wu Q, Zhang X, Feng Z, Wang M, Mao Q (2022) Efficacy and safety of three new oral antiviral treatment (molnupiravir, fluvoxamine and Paxlovid) for COVID-19: a meta-analysis. *Ann Med* 54:516–523. <https://doi.org/10.1080/07853890.2022.2034936>
63. Thakur M, Datusalia AK, Kumar A (2022) Use of steroids in COVID-19 patients: a meta-analysis. *Eur J Pharmacol* 914:174579. <https://doi.org/10.1016/j.ejphar.2021.174579>

Publisher's Note Springer Nature remains neutral with regard to jurisdictional claims in published maps and institutional affiliations.

Springer Nature or its licensor (e.g. a society or other partner) holds exclusive rights to this article under a publishing agreement with the author(s) or other rightsholder(s); author self-archiving of the accepted manuscript version of this article is solely governed by the terms of such publishing agreement and applicable law.